Astron. Astrophys. 334, 571–584 (1998)

ASTRONOMY AND ASTROPHYSICS

On the high frequency polarization of pulsar radio emission

A. von Hoensbroech[1], **J. Kijak**[2,1], **and A. Krawczyk**[2,1]

[1] Max-Planck-Institut für Radioastronomie, Auf dem Hügel 69, D-53121 Bonn, Germany
[2] The Astronomical Centre of Zielona Góra, Lubuska 2, PL-65 265 Zielona Góra, Poland

Received 7 November 1997 / Accepted 27 February 1998

Abstract. We have analyzed the polarization properties of pulsars at an observing frequency of 4.9 GHz. Together with low frequency data, we are able to trace polarization profiles over more than three octaves into an interesting frequency regime. At those high frequencies the polarization properties often undergo important changes such as significant depolarization. A detailed analysis allowed us to identify parameters, which regulate those changes. A significant correlation was found between the integrated degree of polarization and the loss of rotational energy $\dot{E}$.

The data were also used to review the widely established pulsar profile classification scheme of core- and cone-type beams.

We have discovered the existence of pulsars which show a strongly *increasing* degree of circular polarization towards high frequencies.

Previously unpublished average polarization profiles, recorded at the 100m Effelsberg radio telescope, are presented for 32 radio pulsars at 4.9 GHz. The data were used to derive polarimetric parameters and emission heights.

Key words: polarization – radiation mechanisms: non-thermal – radiative transfer – pulsars: general – pulsars: individual: PSR B0144+59; PSR B0355+54

1. Introduction

Polarimetry plays a key role in our understanding of the emission mechanism of pulsars, the ambient conditions in the emission region and the geometrical structure of the magnetic field. Similar to the great variety of profile shapes, the polarimetric features of the radio emission vary strongly from pulsar to pulsar and from frequency to frequency. Virtually every polarization state between totally unpolarized and fully linearly or highly circularly polarized can be found amongst different pulsars and even within one profile. Also the shape of the polarization position angle (hereafter PPA) curve varies between nearly constant, a smooth orderly swing, sudden jumps and nearly chaotic behaviour. The jumps in the PPA–swing often cover precisely 90° and are therefore called orthogonal polarization modes (hereafter OPM, see e.g. Stinebring et al. 1984; Gil & Lyne 1995; Gangadhara 1997).

Nevertheless certain common pulse features have been identified in the past, which lead to different classification attempts (e.g. Backer 1976; Rankin 1983; Lyne & Manchester 1988). It is widely accepted that two general types of profile components can be identified: Those which are radiated from the outer parts of the emission tube as *conal* profile components and those which are usually emitted from the central part as *core*-beams. This classification was initially formulated systematically by Rankin (1983), for a detailed description we refer to that paper, a short summary is given in Sect. 4.1. The identification of these components is mainly (but not only) based on the frequency development of their polarization and their relative intensity. In general this system has proven to be remarkably successful, although in this paper we discuss some groups of pulsars which do not quite fit into this classification scheme.

One common polarimetric feature of most pulsars is the depolarization towards high frequencies (in the following "high frequency" means radio frequencies well above one GHz). Whereas the degree of polarization of pulsars is usually constantly high at low frequencies, it decreases rapidly above a certain frequency (e.g. Manchester 1971; Morris et al. 1981a; Xilouris et al. 1996). This tendency is in contrast to the known properties of other astrophysical objects which have usually stronger polarization at higher frequencies, where the Faraday-depolarization effect is less severe. Therefore, this effect is thought to be inherent to the pulsar magnetosphere, either intrinsic to the emission mechanism or due to a propagation effect within the magnetosphere. The identification of the depolarization mechanism is important as it might help to understand the environmental conditions in the magnetosphere and the relevant physical processes. It is therefore necessary to carry out high frequency observations as we would like to identify parameters which control this effect.

In this paper we also focus on the role of the circular polarization. Theories proposed to explain this type of polarization range from purely intrinsic mechanisms (e.g. Radhakrishnan & Rankin 1990) to pure propagation effects (e.g. Melrose & Stoneham 1977) and combinations of both (e.g. Kazbegi et al. 1991; Naik & Kulkarni 1994). In order to distin-

Send offprint requests to: A. von Hoensbroech, (avh@mpifr-bonn.mpg.de)

guish between the different mechanisms, it is necessary to trace the frequency development of the circular polarization over a large frequency interval. Propagational effects should show a strong frequency dependence.

Whereas the degree of polarization varies strongly with frequency, the measured PPA is very stable over many octaves in frequency. If one allows for the occurrence of OPMs, the PPA swing is therefore thought to reflect the geometry of the pulsar magnetosphere as first noted by Radhakrishnan & Cooke (1969). In some cases it is therefore possible to determine the viewing geometry of a pulsar by fitting the geometry dependent theoretical PPA curve – the rotating vector model (hereafter RVM) – to the measured PPA (the formula for the RVM is given e.g. by Manchester & Taylor (1977)).

Many authors indicate the existence of a radius-to-frequency mapping (hereafter RFM) where the radio emission is narrow band and scales inversely with frequency (e.g. Cordes 1978; Blaskiewicz et al. 1991; Kramer et al. 1997; Kijak & Gil 1997; von Hoensbroech & Xilouris 1997a). The knowledge of the existence and the strength of the RFM is important as it will help to understand the emission physics. It is therefore necessary to determine the emission height above the pulsar surface, where the emission we observe at a certain frequency, originates. Polarimetry provides one method amongst others to calculate this height. This method was proposed by Blaskiewicz et al. (1991) and we have applied it to our data whenever possible (see Sect. 3.2).

Due to their steep radio spectra, pulsars tend to be rather weak sources at centimetre wavelengths. As a result, relatively little published data exists in this part of the spectrum (Morris at al. 1981b; Xilouris et al. 1994; Xilouris et al. 1995; Manchester & Johnston 1995; Xilouris et al. 1996; von Hoensbroech et al. 1997b). In this paper we present the polarimetric properties of 32 weaker pulsars at 4.9 GHz which roughly doubles the number of published polarization profiles at this frequency and allows statistical studies at such a high frequency for the first time.

2. Observations

The observations were carried out at the Effelsberg 100-meter radio telescope of the Max-Planck-Institute für Radioastronomie. The centre frequency was set to 4.85 GHz with a bandwidth of 500 MHz and a system temperature of $T_{\rm sys} \simeq 30$K. The left-hand (LHC) and right-hand circular (RHC) output signals of the secondary-focus receiver were combined and detected in a broad-band multiplying polarimeter in the focus cabin. After an analogue-to-digital conversion using fast voltage-to-frequency converters, the signal was passed down to the pulsar backend where it was recorded synchronously to the topocentric pulsar period. A detailed description of the Effelsberg pulsar observing system (EPOS) can be found in Jessner (1995). The data were then dynamically calibrated using a calibration signal which was injected synchronously to the pulsar period into the waveguide. The full calibration method is described in von Hoensbroech & Xilouris (1997b).

The details of the observations are listed in Table 1.

Table 1. List of observations. The effective Δt is the time resolution, which results from the temporal bin width and the dispersion smearing: $\Delta t = \sqrt{\Delta t^2_{\rm bin} + \Delta t^2_{\rm disp}}$.

PSR	Date [d-m-y]	Period [s]	Pulses No.	eff. Δt [msec]
B0031−07	16-08-95	0.943	600	2.9
B0144+59	08-11-95	0.196	4332	1.4
B0402+61	20-08-95	0.595	1000	2.7
B0450−18	21-08-95	0.549	540	1.8
B0559−05	08-11-95	0.396	5624	3.2
B0611+22	26-09-95	0.335	2244	3.7
B0626+24	28-09-96	0.476	3565	3.4
B0628−28	27-07-95	1.244	2349	5.0
B0818−13	20-08-95	1.238	480	3.1
B0834+06	26-09-95	1.274	1782	2.8
B0906−17	08-11-95	0.402	4255	1.7
B0942−13	08-11-95	0.570	5538	1.3
B1039−19	08-11-95	1.386	1180	3.2
B1254−10	20-08-95	0.617	960	2.2
B1604−00	15-08-95	0.422	700	0.4
B1702−19	26-08-95	0.299	1300	0.8
B1706−16	20-09-95	0.653	1833	1.1
B1737+13	20-08-95	0.803	738	2.5
B1737−30	02-09-91	0.607	960	3.7
B1800−21	16-08-95	0.134	3360	8.5
B1821+05	20-08-95	0.753	779	3.9
B1823−13	18-07-96	0.101	5880	8.4
B1831+04	14-08-95	0.290	2040	3.2
B1839+56	16-08-95	1.653	360	3.7
B1911−04	14-08-95	0.826	720	3.4
B1913+10	21-08-95	0.405	1702	9.2
B1944+17	20-09-95	0.441	1996	2.7
B1952+29	22-08-95	0.427	2800	1.0
B2110+27	21-08-95	2.517	984	5.8
B2111+46	09-11-95	1.015	2854	5.6
B2303+30	21-08-95	1.576	378	3.9
B2334+61	20-08-95	0.495	1200	2.6

3. Results

In this paper we present 32 average polarization profiles for weaker radio pulsars as a result of a large survey at a wavelength of λ= 6.1 cm (Kijak et al. 1998). The polarization diagrams are displayed in Figs. 7 to 10. In Table 2, we list the degrees of linear and circular polarization for each source. Most of the pulsars in our sample show a fairly low degree of polarization, which made the determination of the PPA sometimes uncertain. Therefore the RVM could be fitted only for eight pulsars. The fitted PPA swings are included into the Figs. 7 to 10 for those eight pulsars. The viewing geometry – which is the inclination angle between the rotation axis and the magnetic field axis α, and the "impact angle" between the magnetic field and the line of sight β – was determined for these objects. The results for α and β are listed in columns 2 and 3 of Table 3, respectively, with their estimated

Table 2. Degrees of polarization, averaged over the whole pulse. The corresponding polarization diagrams are displayed in Figs. 7 to 10. $\bar{\Pi}_{\rm L}$ is the linear polarization, $|\bar{\Pi}_{\rm C}|$ and $\bar{\Pi}_{\rm C}$ represent the absolute value and the averaged value of the circular polarization respectively (the convention is *positive* for left-hand and *negative* for right-hand-sense. For B1702-19, values are given for the main pulse (MP) and the interpulse (IP).

PSR	$\bar{\Pi}_{\rm L} \pm \Delta_{\Pi_{\rm L}}$ [%]	$\lvert\bar{\Pi}_{\rm C}\rvert \pm \Delta_{\lvert\Pi_{\rm C}\rvert}$ [%]	$\bar{\Pi}_{\rm C} \pm \Delta_{\Pi_{\rm C}}$ [%]
B0031−07	11 ± 1	8 ± 1	$+8 \pm 1$
B0144+59	11 ± 1	50 ± 1	-49 ± 1
B0402+61	7 ± 4	16 ± 4	-2 ± 6
B0450−18	19 ± 2	8 ± 2	$+7 \pm 4$
B0559−05	40 ± 6	10 ± 3	$+5 \pm 5$
B0611+22	43 ± 8	27 ± 6	$+26 \pm 9$
B0626+24	23 ± 2	9 ± 2	-9 ± 3
B0628−28	2 ± 1	3 ± 1	-3 ± 2
B0818−13	21 ± 4	12 ± 4	-3 ± 6
B0834+06	2 ± 11	23 ± 8	-5 ± 12
B0906−17	4 ± 2	6 ± 2	-2 ± 3
B0942−13	4 ± 8	8 ± 7	$+1 \pm 11$
B1039−19	5 ± 1	8 ± 2	$+6 \pm 2$
B1254−10	20 ± 5	12 ± 4	-8 ± 7
B1604−00	7 ± 1	7 ± 1	-4 ± 1
B1702−19$^{\rm MP}$	37 ± 2	14 ± 2	-10 ± 3
B1702−19$^{\rm IP}$	60 ± 17	17 ± 13	-6 ± 21
B1706−16	18 ± 1	5 ± 1	$+0 \pm 1$
B1737+13	18 ± 3	9 ± 2	$+4 \pm 4$
B1737−30	53 ± 7	59 ± 4	$+59 \pm 5$
B1800−21	71 ± 2	33 ± 1	$+33 \pm 2$
B1821+05	13 ± 2	10 ± 2	-1 ± 3
B1823−13	70 ± 3	42 ± 2	$+42 \pm 2$
B1831+04	15 ± 1	8 ± 1	-1 ± 1
B1839+56	10 ± 2	6 ± 2	$+4 \pm 3$
B1911−04	8 ± 2	7 ± 2	-3 ± 3
B1913+10	4 ± 7	73 ± 10	$+73 \pm 14$
B1944+17	18 ± 2	16 ± 1	-15.0 ± 2
B1952+29	8 ± 1	8 ± 1	$+1 \pm 1$
B2110+27	22 ± 6	17 ± 7	$+4 \pm 10$
B2111+46	22 ± 1	11 ± 1	$+3 \pm 1$
B2303+30	17 ± 2	6 ± 2	$+6 \pm 3$
B2334+61	57 ± 6	18 ± 4	-8 ± 7

errors. These errors are sometimes relatively large due to the ambiguity in the determination of the viewing geometry (see also von Hoensbroech & Xilouris 1997a). However, within our sample of 32 pulsars, there are some particularly interesting ones, which are discussed in the following sections.

3.1. Interesting individual objects

3.1.1. Interpulse: B1702-19

At 4.9 GHz this pulsar is still highly polarized in both its main pulse and interpulse. The main pulse appears to consist of two or three components and is 50% linearly polarized. It shows right and left hand circular polarization. The interpulse is totally linearly polarized but this linear polarization decreases to lower frequencies. Whereas the ratio of interpulse to main pulse intensity increases with frequency up to 1.4 GHz (see Biggs et al. 1988; Biggs 1993; Gould 1994), we find a decrease of this ratio above 1.4 GHz. The geometrical parameters α and β obtained from fitting PPA resemble very much those obtained at lower frequencies using different methods (see Biggs et al. 1988; Lyne & Manchester 1988).

Table 3. Derived geometrical parameters of eight pulsars. α is the inclination angle between the rotation axis and the magnetic field axis, β the *impact angle* between the magnetic field and the line of sight. $r_{\rm pol}$ is the emission height calculated using a polarimetric method (Blaskiewicz et al. 1991), $r_{\rm KG}$ calculated using a relationship proposed by Kijak & Gil (1997), see Eq. 2.

PSR	$\alpha[^\circ]$	$\beta[^\circ]$	$r_{\rm pol}$ [km]	$r_{\rm KG}$ [km]
B0144+59	90 ± 90	0 ± 90	20 ± 70	190 ± 90
B1604−00	90 ± 75	0.2 ± 0.2	380 ± 80	240 ± 80
B1702−19$^{\rm MP}$	86 ± 2	-4 ± 2	300 ± 90	260 ± 80
B1702−19$^{\rm IP}$			310 ± 160	260 ± 80
B1706−16	90 ± 65	-2 ± 1	560 ± 70	330 ± 100
B1737+13	90 ± 86	-2 ± 2	30 ± 280	320 ± 110
B1800−21	90 ± 90	0 ± 90	-40 ± 230	190 ± 50
B2111+46	38 ± 37	-4 ± 4	510 ± 510	320 ± 150
B2334+61	90 ± 88	-8 ± 7	340 ± 540	390 ± 50

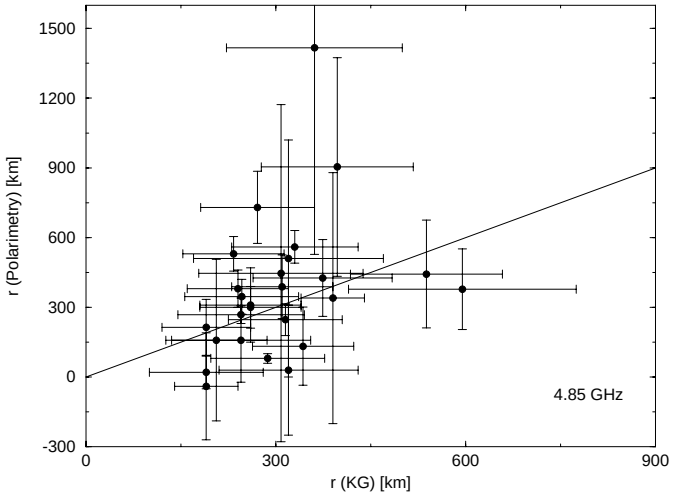

Fig. 1. Comparison of emission heights derived with the polarimetry method ($r_{\rm pol}$) and those derived with an empirical relationship ($r_{\rm KG}$, see text). Those points whose error-bars cut the diagonal are consistent within their one σ errors.

3.1.2. Wide profiles: B1800-21, B1823-13 and B1831-04

With more than 100° width in pulse longitude at this frequency, these pulsars have very wide profiles. PSR B1800-21 is highly polarized and shows one sense of circular polarization. The PPA

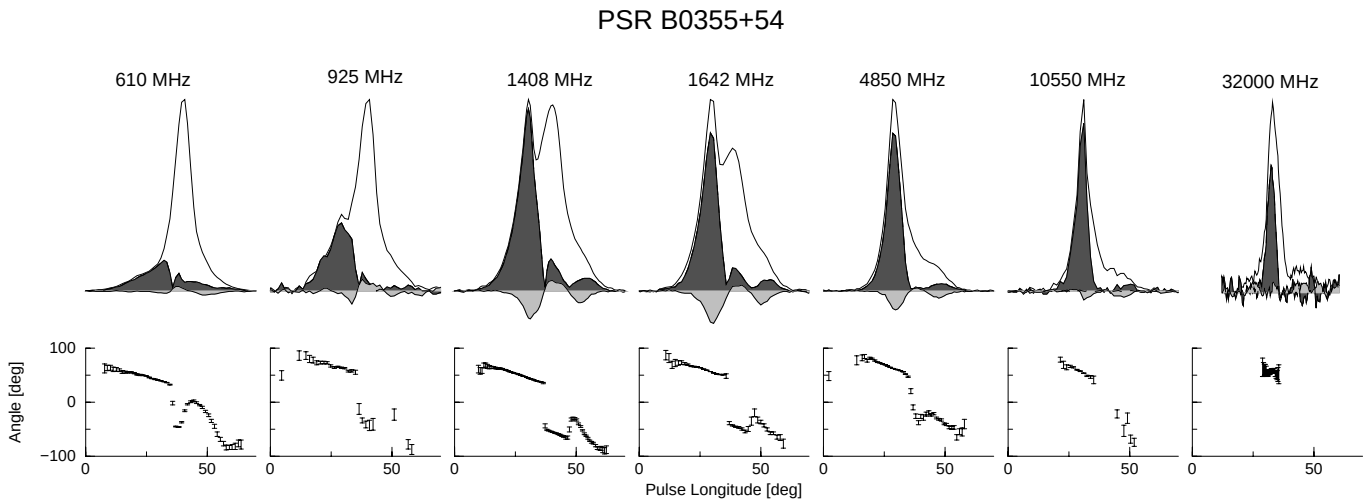

Fig. 2. Polarization profiles of PSR B0355+54 (profiles below 2 GHz are from Gould & Lyne (1998), the others are Effelsberg data. The 32 GHz profile is from Xilouris et al. (1996)). The dark-shaded area represents the linear, the light-shaded area corresponds to the circularly polarized intensity (*positive* = left-hand, *negative* = right-hand). Total power is represented by the unshaded solid line. The first component is highly linearly polarized and becomes increasingly prominent at high frequencies.

follows an S-shaped course through the pulse. PSR B1821-13 is similar to the former one and appears have two or more components in its profile. It is also highly polarized. A detailed discussion on these two pulsars will be given in Sect. 4.1.3. PSR B1831-04 has a multicomponent profile but low polarization.

3.1.3. High circular polarization: B0144+59, B1737-30 and B1913+10

These objects show an unusually high degree of circular polarization ($\geq 50\%$) at 4.9 GHz which is not seen at lower frequencies. A detailed discussion on the frequency development of these pulsars and the consequences of this observation is given in Sects. 4.1.4 and 4.3.

3.2. Geometry and emission altitudes

Radhakrishnan & Cooke (1969) were the first to argue that the magnetic field in the emission region has a dipolar structure and that the PPA corresponds to the projection of the magnetic field line direction on the sky. More recently, Blaskiewicz et al. (1991) demonstrated that the PPA curves behave as predicted in the case of a *vacuo* purely dipolar aligned rotator (Goldreich & Julian 1969). The relativistic model for the RVM (see Blaskiewicz et al. 1991) gives a formula for the calculation of absolute emission heights as

$$r_{\rm em}(\nu) = \frac{c}{4} \cdot \Delta t(\nu) \ , \qquad (1)$$

where Δt is the time lag between the centroid of the total intensity profile and the pulse phase at which the derivative of the PPA curve has its maximum. We calculated the emission altitudes for nine profiles (eight pulsars, one with interpulse) at 4.9 GHz using our polarization data (see Table 3). Together with the emission heights for 17 pulsars from (von Hoensbroech & Xilouris 1997a) at the same frequency and derived using the same method, we compared the results with predictions from the relationship proposed by Kijak & Gil (1997)

$$r_{\rm KG} = (55 \pm 5) \cdot R\, \nu^{-0.21\pm0.07}\, \tau_6^{-0.07\pm0.03} P^{0.33\pm0.05} \ . \qquad (2)$$

$R = 10^4$m is the neutron star radius, ν is the frequency in GHz, τ_6 is the timing age in units of million years and P is pulsar period in seconds. In most cases the results are consistent within the errors (see Fig. 1). This result supports the view that the pulsar high frequency radio emission originates from a region very close to the pulsar surface at a few percent of the light cylinder radius.

4. Discussion

We have analyzed our data together with high frequency data which was already published by von Hoensbroech & Xilouris (1997b) and compared the polarimetric properties to those at lower frequencies. The low frequency data is from Gould & Lyne (1998) and was accessed through the European Pulsar Network (EPN) internet database [1].

4.1. Typical polarimetric types of pulsars

The great variety of pulsars in pulse-shapes and polarization characteristics has always puzzled many researchers. Some authors proposed empirical classification concepts (e.g. Rankin 1983; Lyne & Manchester 1988). These classification schemes are based on the different properties of *core* and *conal* components: The core components are usually located close to the profile centre and tend to show a moderate degree of circular polarization and an unsystematic PPA swing. Cone components

[1] The EPN internet database can be accessed through: *http://www.mpifr-bonn.mpg.de/pulsar/data/*

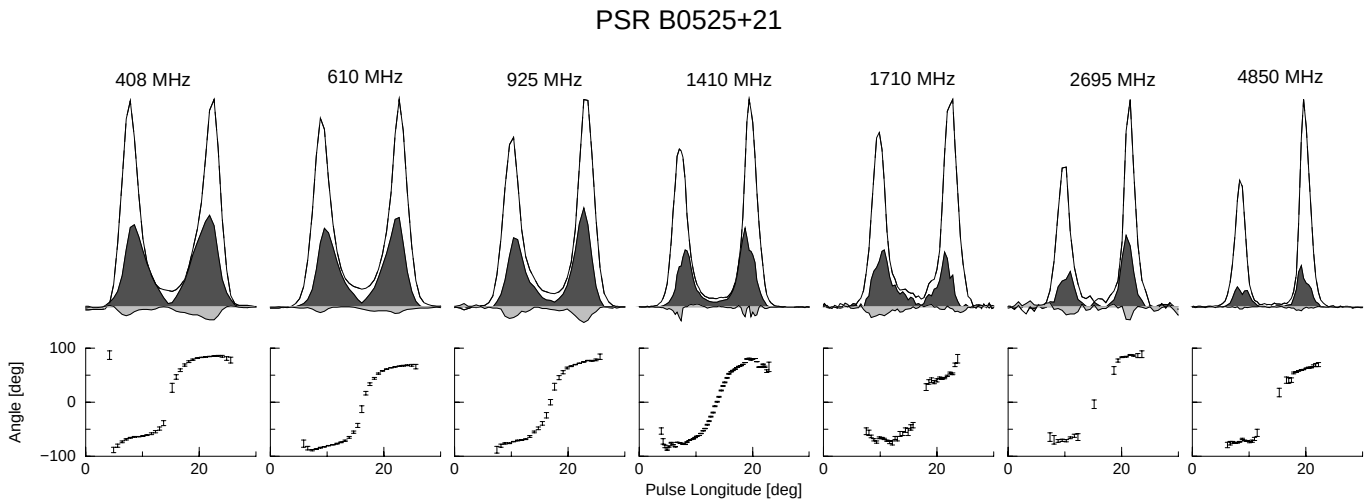

Fig. 3. Frequency development of the polarization profile of PSR B0525+21. (profiles below 1 GHz are from Gould & Lyne (1998), the others are Effelsberg data). For details see Fig. 2. A nice double component profile with an PPA swing which nearly perfectly agrees with the RVM. Significant contributions of circular polarization can be seen below the two intensity peak and correlate well with deviations from the RVM. The narrow profile depolarizes well towards high frequencies.

show hardly any circular and a moderate degree linear polarization. The PPA swing is more systematic and can usually be modelled with the RVM. The spectral index (si in $S \propto \nu^{-si}$) for the core components is higher than for the cone components (see also Kramer et al. 1994). Therefore, at high frequencies cone components become increasingly visible, if not dominant. Finally, core components tend to be more stable and features like mode changing – temporal changes of the average profile – and drifting subpulses – stable subpulse features, which drift systematically with respect to the pulse phase through successive individual pulses, see e.g. Manchester et al. (1975) – are rarely seen for these components.

The shape of a pulse profile then mainly depends on the *impact angle* and on the pulsar-specific *source function*, which represents the (patchy?) filling function of the emitting tube (e.g. Lyne & Manchester 1988; Manchester 1994). If the impact angle is small enough, the line of sight possibly cuts through the central beam and the corresponding core component becomes visible.

Our pulsar sample at 4.9 GHz generally fits well in these concepts. Nevertheless, we find a few groups of objects whose properties differ from what is expected from these classification systems. As these are not just individual objects, but form groups with similar characteristics, it is suggested that additional (or different) effects can play a role for the creation of intensity and polarization profiles of radio pulsars. As some authors already pointed out, there is an evolutionary aspect to keep in mind. So young pulsars tend to be highly polarized (e.g. Melrose 1994) and the cone–dominated ones are usually old (e.g. Rankin 1983).

4.1.1. 0355+54-Type

This group of pulsars, which is represented by the pulsar B0355+54, consists of objects which share the following features: One component is highly linearly polarized ($\Pi_{\rm L} > 60\%$) whereas the rest of the profile shows only little or moderate polarization. The highly polarized component has a flatter spectral behaviour than the profile as a total, thus dominating it at high frequencies. (see Fig. 2). Examples for such pulsars are PSRs B0355+54, B0450+55, B0599−05, B0626+24, B1822−09, B1842+14, B1935+25 and B2224+65. The existence of pulsars with a highly polarized leading component has already been noted in several papers (e.g. Manchester et al. 1980; Morris et al. 1981a), but within this group we find also 2 pulsars where the polarized component is trailing. Interestingly, these pulsars seem to have preferably two main components. They have usually been classified as *half cones* (e.g. Lyne & Manchester 1988; Rankin et al. 1989), meaning that only one half of the polarized cone can be seen. This view has been supported by the fact that the PPA follows a shallow change during the polarized part of the profile (corresponding to an outer part of the emission cone) and a steeper change during the unpolarized component (corresponding to an inner part). The surprising fact is that, if they were really half cones, one would expect to find even a larger number of pulsars with two highly polarized components, enclosing one unpolarized part. We are not aware of any such example, thus this observation puts doubt on the interpretation of these pulsars as half cones.

4.1.2. 0525+21-Type

These are the "textbook"-pulsars. Classified as conal doubles (Rankin 1983) they represent the traditional hollow cone model. The two components are moderately linearly polarized and the PPA follows nearly perfectly the RVM. Between the two components they usually show a core-type bridge (see Fig. 3). Examples for such pulsars are the PSRs B0148−06, B0301+19, B0525+21, B0751+32, B0917+63, B1039−19 and B1938−04. But there are some remarkable facts to mention about these pul-

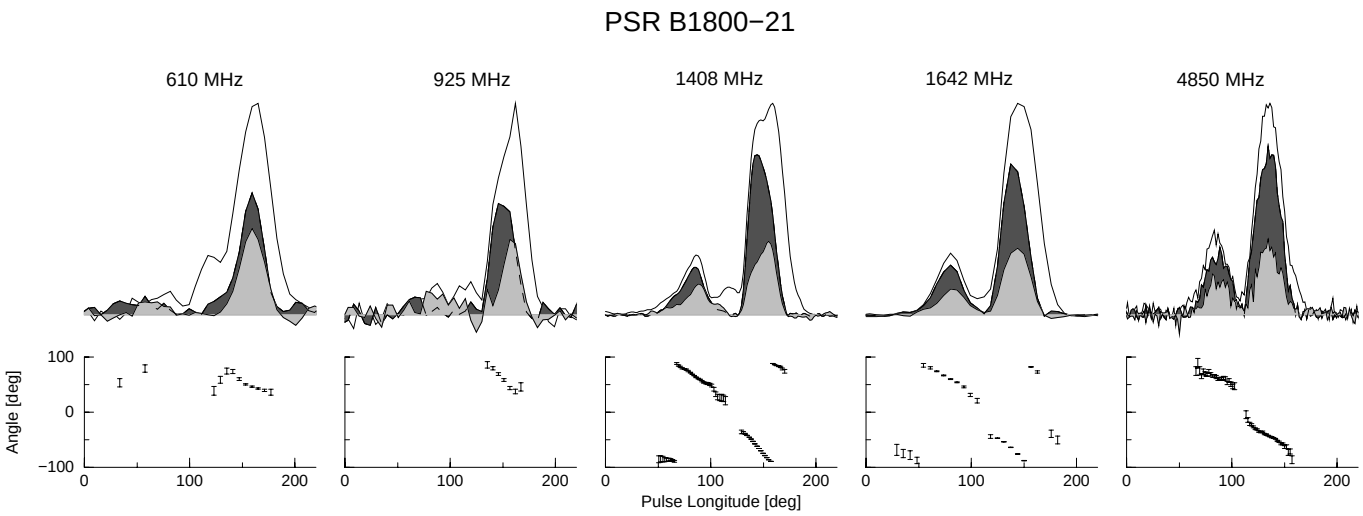

Fig. 4. Frequency development of the polarization profile of PSR B1800−21. (The 4850 MHz profile is Effelsberg data, the other ones are from Gould & Lyne (1998)). For details see Fig. 2. The wide profiles show strong linear and circular polarized contributions over most parts of the pulse which increase towards high frequencies.

sars. They often show a certain degree of circular polarization, which is usually associated with the conal components and not with the bridge (as one would expect from the classification). They depolarize strongly towards high frequencies. As they are usually weak objects with a steep spectral index, it is relatively difficult to obtain high frequency polarization profiles.

Interestingly these pulsars are all relatively old objects which are located close to the "death-line" in the $P - \dot{P}$ diagram. The periods are long and the loss of rotational energy $\dot{E}$ is low. Only few objects of this kind are known. This suggests that the relative geometry of pulsar and observer is only partly responsible for the profile morphology. It seems that a major role – both for the profile morphology and the polarization characteristics – is played by the age τ and therefore by intrinsic pulsar parameters, such as $\dot{E}$, which again determine the ambient plasma conditions (see also Sect. 4.2). The ability to emit polarized high frequency radiation in general, and core emission in particular, is obviously reduced for such pulsars. As these objects are usually also the oldest stars, their profile morphology rather appears to be a (final) evolutionary stage than the product of a random geometry (see also Rankin 1983).

4.1.3. 1800−21-Type

Another remarkable group of pulsars shares the following features: They are young objects with a very high $\dot{E}$, a flat radio spectrum behaviour, X-ray emission and radio-emission over a wide fraction of the pulse period. They are nearly fully polarized, linearly and circularly, and do not show any observable depolarization effects towards high frequencies (see Fig. 4). Examples are the pulsars B1800−21, B1823−13 and B1259−63 (Manchester & Johnston 1995).

The behaviour of these pulsars is difficult to explain within the classification scheme, although parallels to conal double pulsars have been drawn for B1800−21 by Wu et al. (1993) and for B1259−63 by Manchester & Johnston (1995). But there are major differences. The 1800−21-type pulsars are much stronger polarized and show so far no depolarization towards high frequencies, as it seems to occur strongly for the classical conal pulsars (Rankin 1983). The high degree of polarization suggests that competing OPMs are not active in most parts of the profile. So either only one polarization mode is produced, or only one mode can propagate. Other differences are the general properties of these objects (see above). In every respect they are opposite to the classical conal pulsars.

The fact that the polarization characteristics of this group are very unusual and the pulsars share the above mentioned other unusual properties, raises the question that there might be an intrinsic relation between a high $\dot{E}$, a shallow spectrum and a high polarization at high frequencies. We investigate this question in more depth in the following section.

4.1.4. 0144+59-Type

During our high frequency analysis we found five pulsars which show an unusual polarization behaviour. Their degree of circular polarization *increases* strongly with frequency (see Fig. 5). This is in sharp contrast to the "textbook"-sentence: "Pulsars depolarize towards high frequencies". As we regard this effect as critical for the emission physics, we will consider it separately in Sect. 4.3. Here we will just discuss these stars in the light of the classification system.

Looking through published data and our own data, we found five examples for this behaviour and a couple of suspects (the lack of high frequency data makes it difficult to confirm the suspects as members of this group). The clear examples are PSRs B0144+59, B0320+39, B1737−30, B1913+10 and B1914+13. Due to their strong circular polarization these pulsars would be usually classified as core-pulsars, but especially the frequency development of the B0144+59-profile puts doubt on this inter-

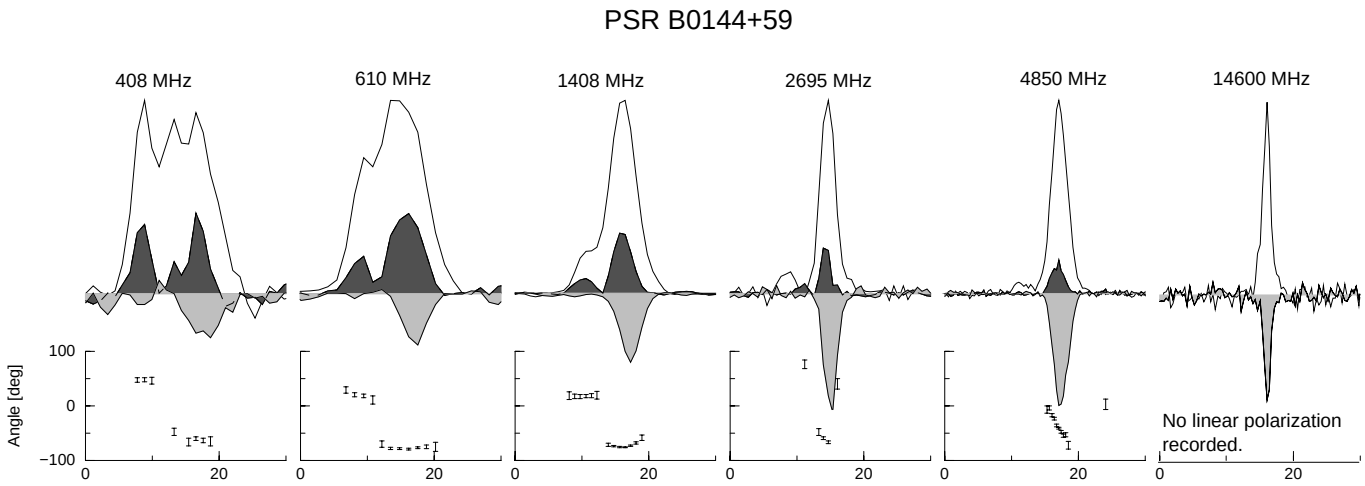

Fig. 5. Frequency development of the polarization profile of PSR B0144+59. The profiles below 2 GHz are from Gould & Lyne (1998), the other profiles are previously unpublished Effelsberg data. Note, that for the 14.6 GHz profile, only circular intensities were measured. The degree of circular polarization increases strongly towards high frequencies. The frequency development of this pulsar is just opposite from what one would expect for a core single ($= S_t$) pulsar.

pretation. At low frequencies, three components can clearly be identified. In opposite behaviour to the prediction of the classification model, the moderately linearly polarized outer components (outriders) weaken towards higher frequencies and the strongly circularly polarized central component dominates the profile. In fact, if the frequency development would be reversed, it would be a perfect example for a core-single (S_t) pulsar.

4.2. Correlations between polarization and other pulsar parameters

An important question within emission physics is, whether the polarization properties correlate with any other pulsar parameters. Some researchers have already noticed that the degree of polarization weakly correlates with $\dot{P}$ and anti-correlates with the period P (Morris et al. 1981a; Gould 1994). But this was done at frequencies < 3 GHz and not very significant. The high frequency range on the other hand is of special interest for this question since the depolarization occurs in this regime. A possible correlation could tell us something about the relevant parameters for the depolarization process (which might actually be essentially the same as the polarizing mechanism). To our knowledge two attempts have already been made to correlate the *depolarization index* (which is the power-law-index of $\Pi_{\rm L} \propto \nu^{\alpha}$) to other pulsar parameters. Using 2.7 GHz data, Morris et al. (1981a) presented indications, that long period pulsars depolarize faster than short period ones. Xilouris et al. (1995) presented an anti-correlation between the depolarization index and the surface accelerating potential $\Phi_{\|} = B_{12}/P^2$ (B_{12} being the surfave magnetic field strength) for 29 pulsars, using 10.6 GHz data. Also during the analysis of our data, it became clear, that highly polarized emission at 4.9 GHz can only be found with short period pulsars. This corresponds to the relationship found by Morris et al. (1981a) at 2.7 GHz.

The degree of polarization therefore seems to correlate more or less significantly with various pulsar parameters. We want to know, with which property the best correlation can be found, applying the following procedure: The two parameters which we can measure with the greatest accuracy are the period P and the period derivative $\dot{P}$. From these parameters we can derive other pulsar properties, such as *characteristic age τ, surface magnetic field B, rotational energy loss $\dot{E}$ and the polar gap accelerating potential* $\Phi_{\|}$. The functional dependency of all these parameters is $\propto P^a \cdot \dot{P}^b$, with different exponents a and b. In order to find a possible correlation with one of the pulsar properties, we correlated the degree of polarization with the above function and varied a and b. The quality of the correlation was then tested using the Pearson-test and the Spearman-rank test (e.g. Press et al. 1992) independently.

Interestingly we found the best correlation not only for one, but for a number of combinations of a and b. The significance of the correlation is 5.5σ, corresponding to a 99.8% probability that the observed correlation is true. All combinations of a and b where this best correlation was found, fulfil the condition: $a/b = -3$. There are two pulsar properties, which match this condition: The rotational energy loss $\dot{E} \propto \dot{P}/P^3$ and the polar gap accelerating potential $\Phi_{\|} \propto (\dot{P}/P^3)^{1/2}$ (see Fig. 6, upper plot).

It is therefore suggested, that these two (intrinsically closely related) parameters strongly influence the polarization properties of the pulsar radio emission.

A similar correlation could not be detected for nearly the same set of pulsars observed at low frequencies (see Fig. 6, lower plot). The integrated degree of polarization seems to be randomly distributed with respect to $\dot{E}$. Comparing to high frequencies, it becomes obvious that mainly highly polarized low-$\dot{E}$ pulsars show significant depolarization, whereas weakly polarized high-$\dot{E}$ pulsars show an increasing degree of polarization to high frequencies. This indicates that pulsars with an

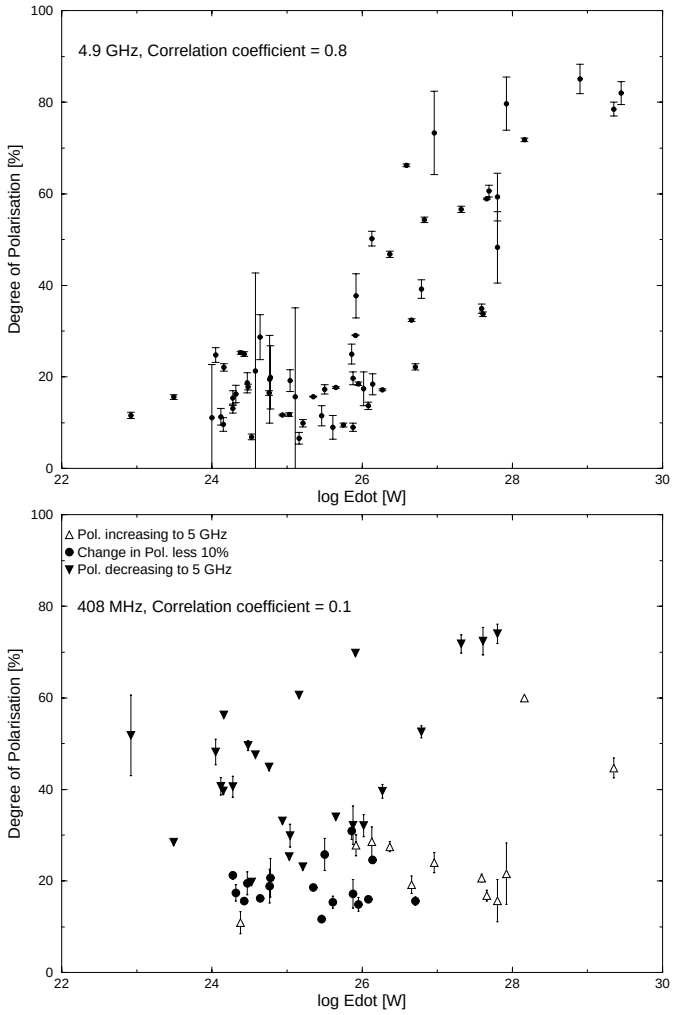

Fig. 6. Plot of the integrated degree of polarization versus the rotational energy loss $\dot{E}$. **Upper plot:** Correlation for 62 pulsars at 4.9 GHz This correlation is highly significant (see text). **Lower plot** Same set of pulsars at 408 MHz (5 pulsars are missing as no low frequency data was available, 2 are recorded at 610 MHz). Obviously no statistically significant correlation is apparent. The degree of polarization *increases* for high $\dot{E}$ pulsars and *decreases* for low $\dot{E}$ pulsars towards high frequencies (see text). The low frequency data were taken from Gould & Lyne (1998).

increasing degree of polarization are not just "outriders", but rather form a systematic group within the pulsar population.

In the following we want to speculate in a straightforward fashion about some possible physical implications of this correlation. Under the assumption that the polarization is not strongly influenced by any outer gap plasma effects, it shows one important fact: When the plasma radiates the radio emission, it somehow "knows" about the accelerating potential inside the polar gap respectively about the loss of rotational energy $\dot{E}$. Until the emission of the observed radiation no processes are allowed, which would result in the loss of this information.

As a possible influence of $\dot{E}$ on the radiating plasma, we regard the following: A high $\dot{E}$ implies a high $\Phi_{\|}$. This again leads to a higher total kinetic energy of the out-flowing plasma. This energy is given by

$$E_{\rm kin} = \bar{\gamma} \cdot N \cdot m_e c^2 \quad \text{with} \quad \bar{\gamma} = \frac{\int n(\gamma) \cdot \gamma \cdot d\gamma}{\int n(\gamma) \cdot d\gamma} \,. \tag{3}$$

$n(\gamma)$ is the energy distribution function of the radiating plasma. In order to increase the total energy, either the number of plasma-particles $N = \int n(\gamma) d\gamma$ or $\bar{\gamma}$ has to increase. To obtain a larger $\bar{\gamma}$, the distribution function $n(\gamma)$ has to be changed either by shifting it to higher energies or by "flattening" the function, thus getting a higher particle population at high γ's. It is unlikely that the whole function can be shifted to much higher energies, as pair-creation and emission of X- and γ-rays will always limit the γ-factor below certain values. In this context it is interesting to note that the X-ray luminosity correlates strikingly well with $\dot{E}$ (Becker & Trümper 1997), which supports the above statement.

We could therefore conclude that either a higher plasma density or a flatter distribution function $n(\gamma)$ implies a higher degree of polarization. There can be two reasons for this:

- If the polarization is an intrinsic property of the emission mechanism it could be concluded that the coherence increases with the plasma density and therefore less independently radiating bunches are superposed and depolarize the radiation. It is also possible that the polarization of the emission mechanism depends on $n(\gamma)$. In this case the degree of polarization would depend on the shape of $n(\gamma)$ insofar as a flatter distribution function results into a higher degree of polarization.
- The polarization may be caused or at least strongly influenced by a propagation effect. The influence would be a different frequency dependent refractive index for the two natural (and orthogonal) propagation modes. The frequency walk of these refractive indices would then depend strongly on the plasma density or $n(\gamma)$.

It might be interesting in this context to point to the fact that there is a slight correlation between the spectral index and $\dot{E}$, such that pulsars with a high $\dot{E}$ often have a flatter spectrum. For example Lorimer et al. (1995) presented an anti-correlation between the spectral index and the characteristic age, which again is anti-correlated with $\dot{E}$. Especially those pulsars which have a high $\dot{E}$ *and* a high polarization (1800−21-type, Sect. 4.1.3) have a very flat spectrum. This corresponds to the behaviour of the highly polarized profile components of the 0355+54-type pulsars (see Sect. 4.1.1), which also have a significantly flatter spectrum than the rest of the profile (see Fig. 2). The spectral behaviour of non-thermal radiation mechanisms mainly depends on the energy distribution function of the emitting particles. If this function is flat, thus more particles have higher energies, then the resulting spectrum is flat as well. Therefore it seems that especially the *shape* of the energy–distribution function $n(\gamma)$ is influenced by $\dot{E}$.

Concluding one should note that these observations suggest an intrinsic relationship between a high $\dot{E}$, a high degree of polarization, and a flat spectrum. This is independent of any core

or conal classification of these stars respectively their profile components. It rather looks as if pulsars with a moderate or high $\dot{E}$ (and therefore also high $\Phi_{\|}$) can develop certain regions on their polar caps, where they direct most of their available energy into the plasma by flattening the distribution function $n(\gamma)$. This plasma then emits a highly polarized radiation with a comparably flatter spectrum than the rest of the radiating plasma. One could even speculate that, if such a region develops, it reduces the plasma energy above other parts of the neutron star, leading to an anti-correlation in the occurrence of certain components in single pulse observations, as it is observed e.g. for PSR B1822−09 (Gil et al. 1994).

4.3. Frequency development of circular polarization

One fundamental piece in the theory of pulsar radiation – where no consensus has been found yet – is the question whether the polarization arises from the emission process itself or whether it is produced by a birefringinal propagation effect (e.g. Melrose & Stoneham 1977; Cheng & Ruderman 1979; Barnard & Arons 1986; McKinnon 1997). The latter case would allow a larger number of considerable emission mechanisms as also processes which are intrinsically *unpolarized* could be considered.

Qualitatively this would correspond to a separation of the original radiation into two orthogonal natural modes which both experience different frequency dependent indices of refraction. A spatial or temporal separation of these two modes could then result into OPMs, a differential absorption into the domination of one mode above the other. The properties of the two modes would be frequency dependent. If the plane of polarization develops an angle to the magnetic field lines during the propagation, the ratio of the two great axis of the polarization ellipse could undergo changes which would result into a transition of linear polarization into circular. Some authors have therefore already suggested, that if propagation effects play a role in the pulsar magnetosphere, they should result into an increasing degree of circular polarization with frequency (Melrose & Stoneham 1977; Cheng & Ruderman 1979). The non-existence of corresponding observations was attributed to a possible competing depolarization mechanism. However authors as Manchester et al. (1980) noted already that some pulsars like Vela show a slightly increasing circular contribution.

The frequency-development of the polarization profile of PSR B0144+59 is to our knowledge the first significant observation of this effect (see Fig. 5 and Sect. 4.1.4). The degree of circular polarization increases constantly with frequency to a very high value ($\Pi_{\rm C} \gtrsim 50\%$), whereas the total degree of polarization ($\Pi_{\rm tot} = \sqrt{\Pi_{\rm L}^2 + \Pi_{\rm C}^2}$) is approximately constant above ~ 1 GHz. It seems unlikely that an intrinsic mechanism other than a propagation effect could result in such a frequency dependence. We therefore suggest that the magnetosphere can have a birefringing quality, which transforms linear polarization into circular, similar to a $\lambda/4$-plate.

Another puzzling aspect about the frequency development of this pulsar is the change of the PPA. One of the basics in the knowledge of pulsar polarization is the stability of the polarization curve – which eventually lead to the conclusion that the shape of this curve is determined by the geometry of the pulsar. The only known qualitative changes are connected to the (frequency dependent) occurrence of OPMs. But in Fig. 5 we observe a smooth steepening of the PPA curve. The same effect is also observed for PSR B1737−30 another pulsar of this class. The classical interpretation for this change would be that the line of sight changes with frequency. An alternative interpretation could be that the same propagation effect which transforms linear into circular polarization, leads to a differential rotation of the plane of polarization.

Unfortunately only little data about such pulsars is available, so no general statement can be drawn yet. But additional observations will be carried out soon.

5. Summary and conclusions

We have analysed average radio pulsar polarization profiles at high frequencies and present 32 previously unpublished pulsar polarization profiles measured at a frequency of 4.9 GHz. The profiles are also available in EPN-format (Lorimer et al. 1998) through the EPN internet database (see Sect. 4). The properties of the whole available set of 4.9 GHz average polarization profiles in general and those of individual pulsars in special were compared to lower frequencies.

Investigating the average polarization profiles of individual pulsars with particular respect to their classification in the scheme of Rankin (1983), we found groups of pulsars which deserve additional attention.

- Some pulsars, such as PSR B0355+54, have components with very different polarimetric and spectral properties within the same profile. One component is nearly fully polarized and has a flatter spectrum than the profile as a whole, thus dominates the profile at high frequencies. The rest of the profile is hardly polarized and dominates only at low frequencies. As all eight pulsars which form this group so far, show a similar frequency-dependence, it is suggested that an intrinsic correlation exists between a high degree of polarization and a flat spectrum. All these pulsars have been classified as half-cones. Although this classification is tempting, it is important to note that not a single full-cone with similar properties could be found. This indicates that a more general process takes place than just an occasional lack of flux at the position where the line of sight cuts the cone for the second time.
- There are three young pulsars (B1800-21, B1823-13 and B1259-63) with a very high loss of rotational energy $\dot{E}$ and a very flat spectrum. These pulsars are nearly fully polarized and do not show any significant depolarization. This behaviour shows similarities to the above mentioned highly polarized components of the 0355-like pulsars. Both groups show a correlation between high polarization and a flat spectrum.
- We found a number of objects which show a circular polarization, which strongly *increases* with frequency. This is in

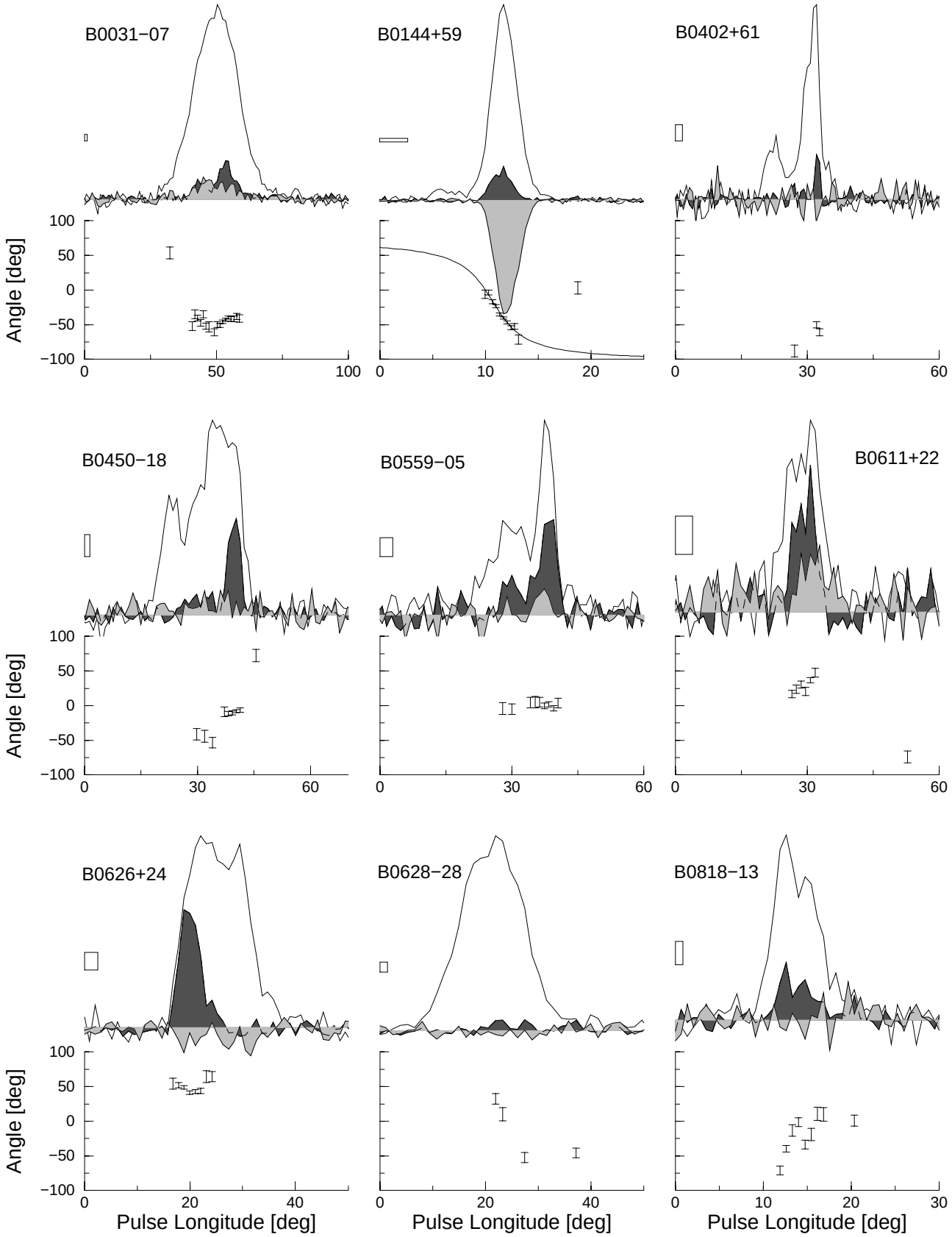

Fig. 7. Pulsar polarization profiles at 4.85 GHz. The dark-shaded area represents the linear, the light-shaded area corresponds to the circularly polarized intensity (*positive* $\hat{=}$ left-hand, *negative* $\hat{=}$ right-hand). Total power is represented by the unshaded solid line. The error-box has a height of 2 σ and a width corresponding to the effective time-resolution (see caption of Table 1). When it was possible, the RVM was fitted to the angle (e.g. for B0144+59).

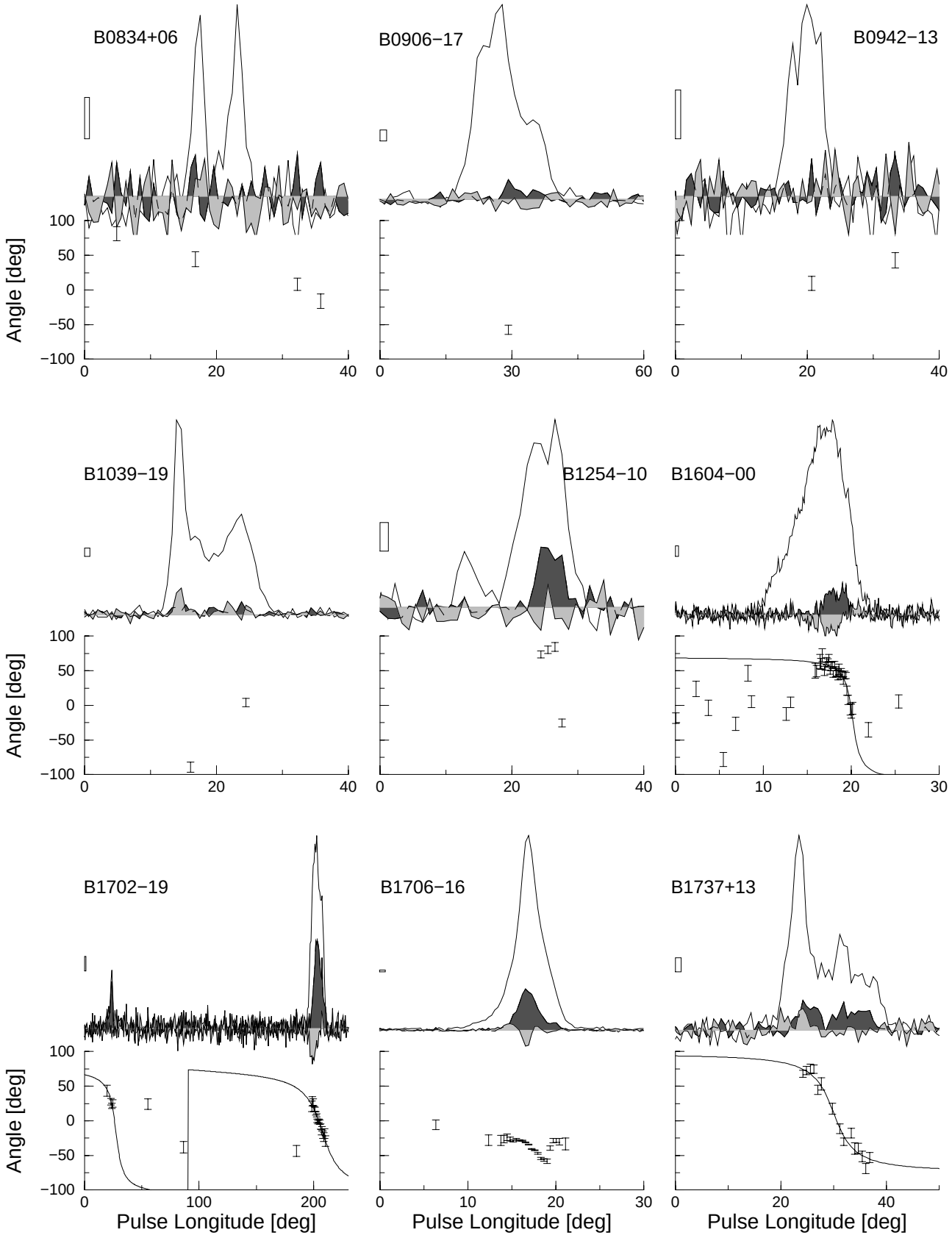

Fig. 8. Pulsar polarization profiles at 4.85 GHz. For details see caption of Fig. 8.

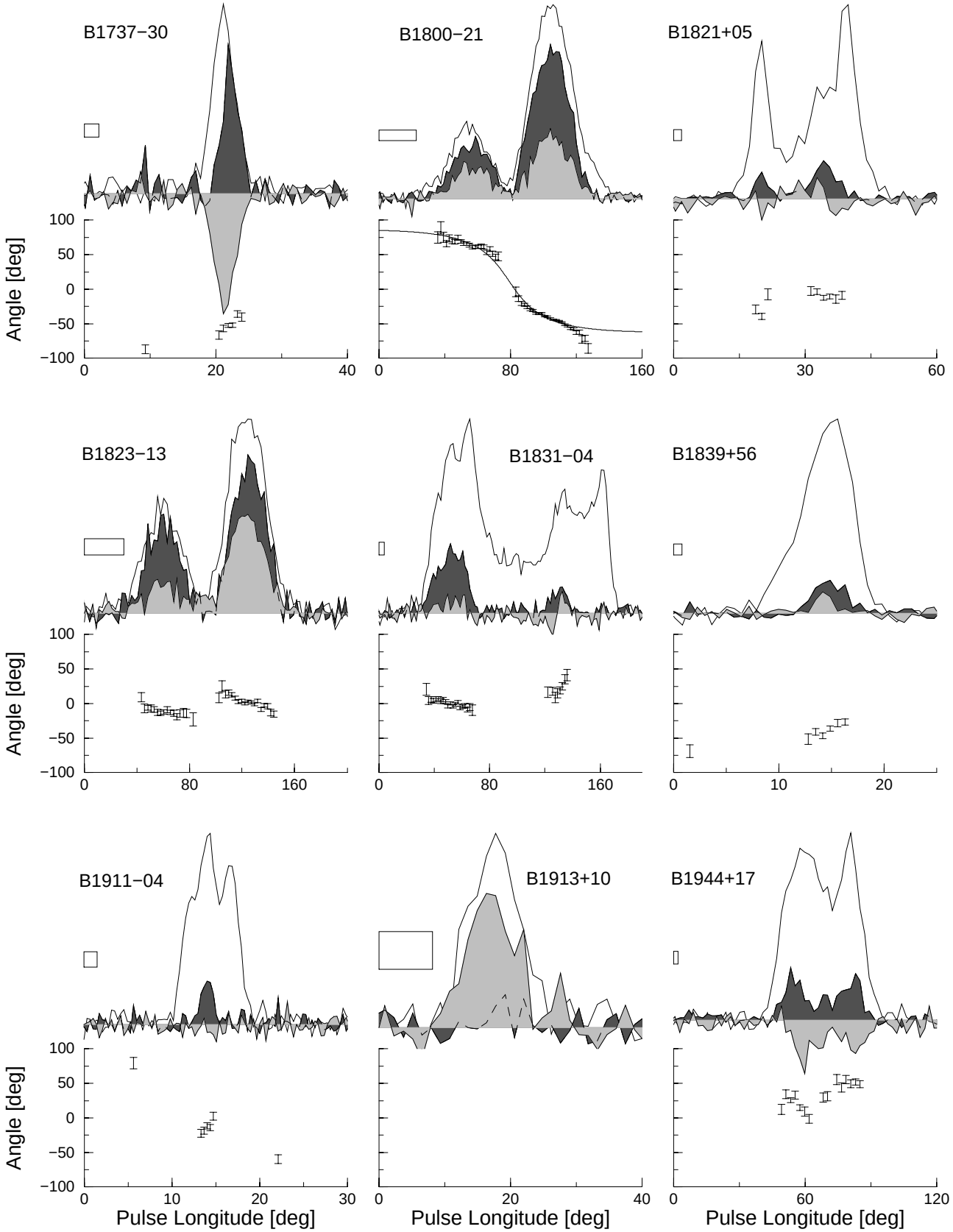

Fig. 9. Pulsar polarization profiles at 4.85 GHz. For details see caption of Fig. 8.

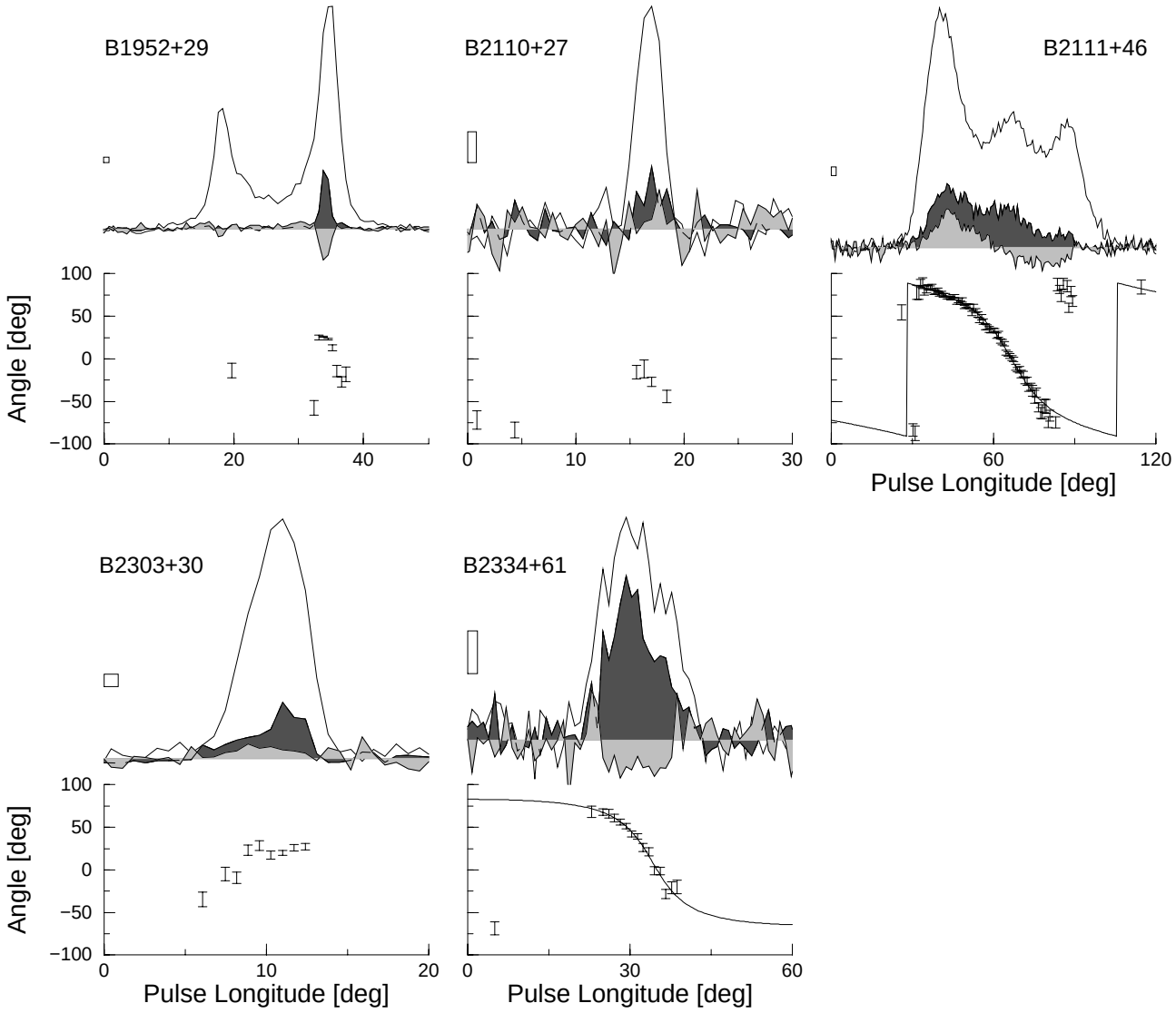

Fig. 10. Pulsar polarization profiles at 4.85 GHz. For details see caption of Fig. 8.

sharp contrast to the known frequency-dependence of pulsar polarization. As the linear polarization decreases simultaneously, it is suggested that a propagation-effect similar to a $\lambda/4$-plate is active. If confirmed, this could indicate, that propagation effects influence the polarization within the magnetosphere. Additionally, these pulsars fit hardly into the classification scheme. PSR B0144+59 for instance shows precisely the opposite frequency-development to a S_t-pulsar (see Fig. 5).

We would like to point out again the possible role of pulsar evolution on the polarization profile. Within the empirical model for pulsar emission, the profile shape and the polarization properties is nearly exclusively determined by the viewing geometry of pulsar and line of sight and the activity in the different parts of the magnetosphere. But, as it was already noted by Rankin (1983), the classical conal double pulsars (the "textbook-pulsars", 0525+21-type) are without exception very old stars which lie close to the "death-line" in the $P-\dot{P}$-diagram. Contrarily the $1800-21$-like pulsars mentioned above are very young pulsars with very different properties. For future work it appears to be important to focus stronger on the role of evolution for polarization profile shapes.

Analysing the general properties of pulsar polarization profiles at this frequency of 4.9 GHz, we found a significant correlation between the total degree of polarization with $\dot{E}$ and the $\Phi_{\|}$ at the polar gap respectively (see Fig. 6, upper plot). Such a correlation does not exist at lower frequencies. The pulsars at low frequencies rather form groups which have a decreasing (highly polarized, low $\dot{E}$ pulsars) and an increasing (weakly polarized, high $\dot{E}$ pulsars) degree of polarization to high frequencies. Observations at high radio frequencies therefore yield additional information on the emission physics which is not seen at lower frequencies. This correlation confirms the relation between the depolarization index and $\Phi_{\|}$ at 10.5 GHz, which was presented by Xilouris et al. (1995).

The large differences in the degree of polarization between individual pulsars indicate that the ambient physical conditions in the respective emitting region differ significantly among them. As we can see from the correlation, this depends on $\dot{E}$. $\dot{E}$ again is closely correlated to the polar gap $\Phi_{\|}$. As a high degree of polarization seems to be correlated to a flatter spectrum (see above), we speculate that a high $\Phi_{\|}$ could induce a flatter energy distribution function of the radiating plasma.

Acknowledgements. We would like to thank R. Wielebinski, R.T. Gangadhara, A. Jessner, M. Kramer, H. Lesch, D. Lorimer, W. Sieber and K.M. Xilouris for support and helpful comments on this paper. For their help with observation we thank O. Doroshenko and C. Lange. We also thank A.G. Lyne and M. Gould for providing us with lower frequency polarimetry data through the EPN internet database (supported by the European Commission under the HCM Network Contract Nr. ERB CHRX CT960633, i.e. the *European Pulsar Network*). This paper was partially supported by the Polish State Committee for Scientific Research Grant 2 P03D 015 12.

References

Backer D.C., 1976, ApJ 209, 895
Barnard J.J., Arons J., 1986, ApJ 302, 138
Becker W., Trümper J., 1997, A&A 326, 682
Biggs J.D. 1993, Isolated Pulsars, Proc. of the Los Alamos Workshop, Cambridge University Press, p. 197
Biggs J.D., Lyne A.G., Hamilton P.A. 1988, MNRAS 235, 255
Blaskiewicz M., Cordes J.M., Wasserman I., 1991, ApJ, 370, 643
Cheng A.F., Ruderman M.A., 1979, ApJ 229, 348
Cordes J.M., 1978, ApJ 222, 1006
Gangadhara R.T., 1997, A&A 327, 155
Gil J., Lyne, A.G., 1995, MNRAS 276, L55
Gil J., Jessner A., Kijak J. et al., 1994, A&A 282, 45
Goldreich P., Julian W.H., 1969, ApJ 157, 869
Gould D.M., 1994, PhD-Thesis, University of Manchester
Gould D.M., Lyne A.G., 1998, MNRAS submitted
von Hoensbroech A., Xilouris K.M., 1997a, A&A 324, 981
von Hoensbroech A., Xilouris K.M., 1997b, A&AS 126, 121
Jessner A., 1995, Proc. SPIE, 2479, 79, Telescope Control Systems, Ed. P.T. Wallace
Kazbegi A.Z., Machabeli G.Z., Melikidze G.I., 1991, MNRAS 253, 377
Kijak J., Gil J., 1997, MNRAS 288, 631
Kijak J., Kramer M., Wielebinski R., Jessner A., 1998, A&AS 127, 153
Kramer M., Wielebinski R., Jessner A., Gil J.A., Seiradakis J.H., 1994, A&AS 107, 515
Kramer M., Xilouris K.M., Jessner A. et al., 1997, A&A 322, 846
Lorimer D.R., Yates J.A., Lyne A.G., Gould D.M., 1995, MNRAS 273, 411
Lorimer D.R., Jessner A., Seiradakis J.H. et al., 1998, A&A in press
Lyne A.G., Manchester R.N., 1988, MNRAS 234, 477
Manchester R.N., 1971, ApJS 23, 283
Manchester R.N., 1994, JApA 16, 107
Manchester R.M., Johnston S., 1995, ApJ 441, L65
Manchester R.N., Taylor J.H., 1977, Pulsars, Freeman, San Francisco
Manchester R.N., Taylor J.H., Huguenin G.R., 1975, ApJ 196, 83
Manchester R.N., Hamilton P.A., McCulloch P.M. 1980, MNRAS 192, 153
McKinnon M.M., 1997, ApJ 475, 763
Melrose D.B., 1994, JApA 16, 137
Melrose D.B., Stoneham R.J., 1977, Proc. ASA 3, 120
Morris D., Graham A.D., Sieber W., 1981a, A&A 100, 107
Morris D., Graham A.D., Sieber W., Bartel N., Thomasson P., 1981b, A&AS 46, 421
Naik P.V., Kulkarni V.H., 1994, Ap&SS 218, 13
Press W.H., Teukolsky S.A., Vetterling W.T., Flannery B.P., 1992, Numerical Recipes, Cambridge University Press
Radhakrishnan V. Cooke D.J. 1969, Astrophys. Lett. 3 225
Radhakrishnan V. Rankin J.M., 1990, ApJ 352, 258
Rankin J.M. 1983, ApJ 274, 333
Rankin J.M. Stinebring D.R., Weisberg J.M., 1989, ApJ 346, 869
Stinebring D.R., Cordes J.M., Rankin J.M. Weisberg J.M., Boriakoff W., 1984, ApJS 55, 247
Wu X., Manchester R.N., Lyne A.G., Qiao G., 1993, MNRAS 261, 630
Xilouris K.M., Kramer M., Jessner A., Wielebinski R., 1994, A&A 288, L17
Xilouris K.M., Seiradakis J.H., Gil J., Sieber W., Wielebinski R., 1995, A&A 293, 153
Xilouris K.M., Kramer M., Jessner A. et al., 1996, A&A 309, 481